Received: 25 July 2023 | Accepted: 15 November 2023

DOI: 10.1111/jpy.13416

RESEARCH ARTICLE

The requirement for external carbonic anhydrase in diatoms is influenced by the supply and demand for dissolved inorganic carbon

Matthew Keys[1] | **Brian Hopkinson**[2] | **Andrea Highfield**[1] | **Abdul Chrachri**[1] | **Colin Brownlee**[1] | **Glen L. Wheeler**[1]

[1]Marine Biological Association, The Laboratory, Plymouth, UK

[2]Department of Marine Sciences, University of Georgia, Athens, Georgia, USA

Correspondence
Matthew Keys and Glen L. Wheeler, Marine Biological Association, The Laboratory, Citadel Hill, Plymouth PL1 2PB, UK.
Email: matkey@mba.ac.uk and glw@mba.ac.uk

Funding information
Natural Environment Research Council, Grant/Award Number: NE/T000848/1

Editor: P.G. Kroth

Abstract

Photosynthesis by marine diatoms contributes significantly to the global carbon cycle. Due to the low concentration of CO_2 in seawater, many diatoms use extracellular carbonic anhydrase (eCA) to enhance the supply of CO_2 to the cell surface. While much research has investigated how the requirement for eCA is influenced by changes in CO_2 availability, little is known about how eCA contributes to CO_2 supply following changes in the demand for carbon. We therefore examined how changes in photosynthetic rate influence the requirement for eCA in three centric diatoms. Modeling of cell surface carbonate chemistry indicated that diffusive CO_2 supply to the cell surface was greatly reduced in large diatoms at higher photosynthetic rates. Laboratory experiments demonstrated a trend of an increasing requirement for eCA with increasing photosynthetic rate that was most pronounced in the larger species, supporting the findings of the cellular modeling. Microelectrode measurements of cell surface pH and O_2 demonstrated that individual cells exhibited an increased contribution of eCA to photosynthesis at higher irradiances. Our data demonstrate that changes in carbon demand strongly influence the requirement for eCA in diatoms. Cell size and photosynthetic rate will therefore be key determinants of the mode of dissolved inorganic carbon uptake.

KEYWORDS

bicarbonate uptake (HCO_3^-), CO_2 diffusion, diatom, diffusive boundary layer (DBL), dissolved inorganic carbon (DIC), external carbonic anhydrase (eCA)

INTRODUCTION

Diatoms are a diverse group of phytoplankton and are particularly prominent in productive marine waters where they are often the dominant photoautotrophs. This results in their significant contribution to marine biogeochemical cycles (Falkowski et al., 2004), as much as 40% of marine primary productivity (Nelson et al., 1995) and up to 20% of global primary productivity (Armbrust, 2009). To support photosynthesis, diatoms acquire dissolved inorganic carbon (DIC) from seawater, and like many other marine phytoplankton, they are strongly reliant on CO_2-concentrating mechanisms (CCMs) to maintain high photosynthetic rates

Abbreviations: AZ, acetazolamide; BZA, benzolamide; CA, carbonic anhydrase; CCM, CO_2 concentrating mechanism; CO_2, carbon dioxide; CO_3^{2-}, carbonate; DBL, diffusion boundary layer; DIC, dissolved inorganic carbon; eCA, external carbonic anhydrase; H^+, hydrogen ion; HCO_3^-, bicarbonate; iCA, internal carbonic anhydrase; O_2, oxygen; PFD, photon flux density; pH, potential of hydrogen; P_{rel}, relative photosynthetic rate; SGR, specific growth rate.

due to the low CO_2 concentration in present-day oceans (Tortell, 2000). Carbon dioxide (the substrate for carbon fixation by the enzyme ribulose-1,5-bisphosphate carboxylase/oxygenase, RuBisCO) makes up <1% of DIC in seawater (Zeebe & Wolf-Gladrow, 2001). Oceanic CO_2 concentrations range between ~10 and 25 μM (typically around ~10 μM in temperate waters), which is significantly lower than the >50 μM required to saturate diatom RuBisCO and to prevent the competing oxygenase reaction due to RuBisCO's low specificity for CO_2 (Hopkinson et al., 2016). Although CO_2 is often the preferred substrate for uptake, the other forms of DIC, bicarbonate (HCO_3^-) and carbonate (CO_3^{2-}), are present in seawater at concentrations greatly exceeding CO_2. Many phytoplankton can therefore utilize HCO_3^-, either by direct uptake of HCO_3^- or via the conversion of HCO_3^- to CO_2 (Martin & Tortell, 2006; Rost et al., 2003). The enzyme extracellular carbonic anhydrase (eCA) catalyzes the otherwise slow interconversion of HCO_3^- to CO_2 at the cell surface of phytoplankton, and the CO_2 generated can then be taken up for photosynthesis by diffusion (Shen & Hopkinson, 2015; Wolf-Gladrow & Riebesell, 1997). Consequently, there are three primary routes for DIC uptake by diatoms: (i) diffusive entry of CO_2 from the low concentration of CO_2 in seawater, (ii) direct HCO_3^- uptake, and (iii) eCA-catalyzed CO_2 diffusion (Figure 1). As the uncatalyzed conversion of HCO_3^- to CO_2 is slow, models indicate that the diffusion of CO_2 alone is unable to support the rates of photosynthesis exhibited by larger phytoplankton species (Reinfelder, 2011; Wolf-Gladrow & Riebesell, 1997). Many diatoms have the capacity to operate all three uptake routes; however, there is considerable variability among species in the relative proportions of DIC taken up as CO_2 or HCO_3^- (Martin & Tortell, 2008). Carbon dioxide entry into diatoms occurs via passive diffusion due to the relative permeability of the plasma membrane to this small uncharged molecule, whereas uptake of the much more abundant HCO_3^- requires the activity of dedicated membrane transporters (Nakajima et al., 2013). Although eCA appears to be ubiquitous in centric diatoms (Shen & Hopkinson, 2015), the presence of eCA in many other taxa, such as pennate diatoms, haptophytes (Nimer et al., 1994, 1997; Rost et al., 2003), and dinoflagellates, (Nimer, Brownlee, & Merrett, 1999; Nimer, Ling, et al., 1999; Rost et al., 2006) is much more variable. This suggests that eCA is particularly important for photosynthetic CO_2 uptake in centric diatoms.

There is significant diversity in diatom size and morphology, ranging over three orders of magnitude in cell diameter and five orders of cell volume (Wu, Jeans, et al., 2014). Larger cells have a lower surface area to volume ratio, and modeling studies predict that the diffusive boundary layer (DBL) around large cells is likely to restrict the diffusion of nutrients and CO_2 to the cell surface (Finkel et al., 2009). Diffusive uptake of CO_2 can

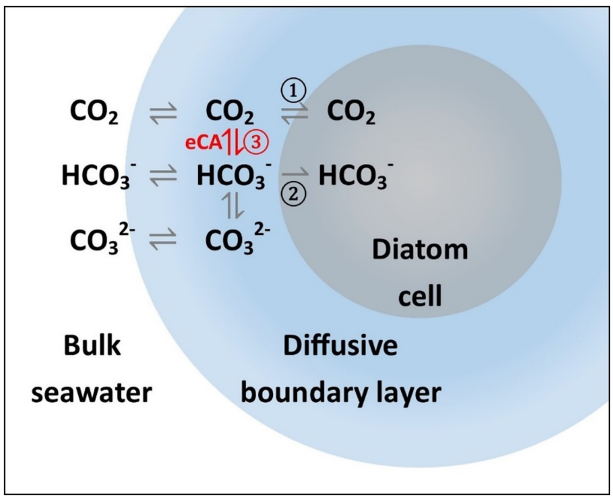

FIGURE 1 Routes for DIC uptake by diatoms. The three primary routes for DIC uptake by diatoms: (1) CO_2 diffusion, (2) direct HCO_3^- uptake, and (3) eCA-catalyzed CO_2 diffusion. CO_2 entry occurs by passive diffusion due to the permeability of the plasma membrane to this small uncharged molecule, whereas HCO_3^- uptake requires the activity of dedicated membrane transporters. The enzyme extracellular carbonic anhydrase (eCA) catalyzes the otherwise slow conversion of HCO_3^- to CO_2, increasing the cell surface CO_2 concentration for subsequent photosynthetic uptake. To investigate changes in the flux of DIC at the cell surface we positioned microelectrodes directly against the frustule, as close to the plasma membrane as is physically possible without damaging cells and impacting cell physiology.

only occur if the cell is able to maintain an inward gradient for CO_2 across the plasma membrane, which is a much greater problem for a large cell with a significant DBL (Gavis & Ferguson, 1975; Reinfelder, 2011; Wolf-Gladrow & Riebesell, 1997). Therefore, larger diatoms overcome diffusive limitation of CO_2 either by direct HCO_3^- transport or by use of eCA to increase the supply of CO_2 at the cell surface. There is an energetic cost associated with direct HCO_3^- transport by dedicated transporters, whereas movement of CO_2 across the plasma membrane occurs by diffusion, and eCA only represents a relatively small proportion of the cellular nitrogen budget (0.1%–0.3% of total cellular nitrogen; Shen & Hopkinson, 2015). The photosynthetic capacity of larger diatoms would deplete CO_2 substantially at the cell surface in the absence of eCA, leading to CO_2 limitation (Riebesell et al., 1993). Carbon dioxide diffusion in smaller diatoms (with associated smaller DBLs) is sufficiently rapid so as not to deplete cell surface CO_2, even in the absence of eCA (Wolf-Gladrow & Riebesell, 1997). Consequently, for larger diatoms the energetic benefit of reducing the CO_2 gradient within the DBL relative to the surrounding bulk seawater may outweigh the costs of producing eCA. External carbonic anhydrase is present in some smaller diatoms, although evidence suggests that it is only induced to support photosynthetic CO_2 uptake at very low DIC concentrations (Hopkinson et al., 2013; Samukawa

et al., 2014). The small diatom *Chaetoceros muelleri* has been observed to increase eCA activity with decreasing DIC in culture, which may help contribute to this species's reported dominance and persistence in phytoplankton blooms (Smith-Harding et al., 2017).

Using the isotope disequilibrium technique to discriminate between HCO_3^- and CO_2 uptake, Martin and Tortell (2008) reported high variability in both direct HCO_3^- uptake and eCA expression among 17 marine diatoms with different cell morphologies. The fraction of HCO_3^- transport ranged from 40% to 95% of total DIC uptake, and a 10-fold range in eCA catalytic enhancement was observed. No correlation was determined between eCA activity and cell size or carbon demand:supply; however, a positive correlation was observed between eCA activity and HCO_3^- uptake. Similar correlations have been recorded in marine diatom studies using membrane-inlet mass spectrometry (MIMS), leading to the proposal that the primary role of eCA is not to enhance cell surface CO_2 but to assist HCO_3^- uptake by scavenging CO_2 leaking out of the cell (Burkhardt et al., 2001; Trimborn et al., 2008, 2009). However, a detailed study of the effects of eCA on cell boundary layer chemistry in *Thalassiosira pseudonana* and *T. weissflogii* supported the proposed role of eCA in CO_2 supply (Hopkinson et al., 2013). This study determined that eCA activity specifically responded to low CO_2 rather than to changes in pH or HCO_3^- and that the rates of eCA activity were optimal for maintaining cell surface CO_2 concentrations near those in the bulk seawater solution. In contrast, model simulations of the proposed alternative role for eCA in the recovery of diffusive CO_2 loss during HCO_3^- uptake determined that eCA had minimal effects on this process (Hopkinson et al., 2013). More recently, eCA activity in six-centric diatoms spanning a broad range of cell sizes was assessed (Shen & Hopkinson, 2015). Carbon fixation rates were quantified with and without an eCA inhibitor to assess the contribution of eCA to carbon acquisition. No relationship was established between the extent of eCA inhibition on reducing photosynthetic rates and cell size; however, photosynthesis in the smallest diatoms (<4 μm radius) was only affected at a very low CO_2 concentration (1.2 μM). In contrast, photosynthesis was negatively affected in some of the larger diatoms tested at typical seawater CO_2 concentrations (8.5 μM) when eCA was inhibited. However, it has been suggested that among-species comparisons may hamper discrimination between cell size and other covarying factors. To account for this potential complication Malerba et al. (2021) evolved a 9.3-fold difference in the cell volume of *Dunaliella tertiolecta* using artificial selection. The authors found that larger *D. tertiolecta* cells upregulated CCMs, which enhanced DIC uptake with higher CO_2 affinity and eCA activity.

Although it is proposed that eCA activity acts to alleviate the depletion of CO_2 within the DBL, there is a paucity in direct measurements of carbonate chemistry within the DBL surrounding phytoplankton cells. Microelectrode measurements of the DBL surrounding multicellular organisms such as the coralline macroalgae *Sporolithon durum* and calcifying macroalgae *Halimeda discoidea* demonstrated a significant rise in pH associated with photosynthetic uptake of DIC (de Beer & Larkum, 2001; Hurd et al., 2011). Similarly, microelectrode measurements of pH at the cell surface of the large diatom, *Coscinodiscus wailesii* demonstrated significant light-activated increases in pH (Kühn & Raven, 2008; Liu et al., 2022), and the smaller diatom *Thalassiosira weissflogii* also exhibited light-activated pH increases at the cell surface (0.4 units higher than surrounding bulk seawater pH), measured with a cell-bound, pH-sensitive fluorescent dye (Milligan et al., 2009). Using microelectrodes to simultaneously measure pH and CO_3^{2-} at the cell surface of the large diatom *Odontella sinensis*, Chrachri et al. (2018) observed rapid and substantial increases in both measured parameters that were light-activated during photosynthesis. By applying eCA inhibitors during microelectrode measurements, the authors showed that carbonate chemistry in the microenvironment around this large diatom is strongly influenced by photosynthetic DIC uptake and that eCA plays a major role in this process. The light-activated elevations in pH and CO_3^{2-} were significantly decreased following inhibition of eCA, showing definitively that the primary role of eCA is to increase the supply of CO_2 to the diatom cell surface by catalyzing its conversion from HCO_3^-.

Many previous studies of eCA activity in phytoplankton have demonstrated that the activity of the enzyme is induced by low concentrations of CO_2 in seawater (Burkhardt et al., 2001; Chen & Gao, 2003; Elzenga et al., 2000; Iglesias-Rodriguez & Merrett, 1997; John-Mckay & Colman, 1997). These experiments are typically performed at saturating light to facilitate comparison between species (Chrachri et al., 2018; Martin & Tortell, 2006; Moroney et al., 1985; Rost et al., 2003). However, this means we have limited knowledge of the contribution of eCA to photosynthesis under lower light levels. In nature, light fluctuates both temporally and spatially, and light availability has long been shown to affect phytoplankton biomass in the oceans (Mitchell et al., 1991; Ryther, 1956). This is important since the growth and photosynthesis of diatoms commonly proceed under the condition of light limitation when photosynthetically driven carbon demands are likely at their lowest (Mitchell et al., 1991; Raven & Falkowski, 1999; Sunda & Huntaman, 1997). Indeed, light intensity has recently been shown to control the magnitude of pH elevation at the cell surface of the large diatom *Odontella sinensis* (Chrachri et al., 2018). Similarly, progressive increases in light intensities from 15 to 180 μmol photons $\cdot$ m^{-2} $\cdot$ s^{-1} resulted in sequential pH elevations within the cell

surface boundary layer of *Chlamydomonas* sp., followed by a decrease in pH after 2 min due to photoinhibitory processes (Liu et al., 2022).

We therefore investigated the contribution of eCA to photosynthesis in three centric diatom species of contrasting cell sizes under a range of ecologically relevant irradiance levels at typical seawater DIC values. We selected strains of *Coscinodiscus granii*, *Thalassiosira punctigera*, and *Skeletonema dohrnii* that were isolated from the western English Channel (Station L4). These genera have previously been shown to possess eCA (Shen & Hopkinson, 2015; Chen & Gao, 2003; Martin & Tortell, 2008; Nimer et al., 1998; Nimer, Brownlee, & Merrett, 1999; Nimer, Ling, et al., 1999; Rost et al., 2003; Trimborn et al., 2009). We determined optimal irradiance levels for growth and measured rates of photosynthetic O_2 evolution in the presence and absence of eCA in cultures and at the single-cell level. We aimed to establish whether larger diatom species, with associated larger DBLs, exhibit greater requirements for eCA and the extent to which these requirements were dependent on the relative demand for DIC driven by changes in irradiance.

MATERIALS AND METHODS

Phytoplankton strains and culture conditions

Coscinodiscus granii (strain PLY8536), *Thalassiosira punctigera* (strain PLY8538), and *Skeletonema dohrnii* (PLY612) were obtained from the Plymouth Culture Collection of Marine Microalgae. All strains were isolated from seawater samples collected from station L4, western English Channel. *Coscinodiscus granii* was isolated in November 2020; *T. punctigera* was isolated in March 2017; and *S. dohrnii* was isolated in June 2003. Stock cultures were maintained in aged filtered sterile seawater with f/2 media with 100 μM silicate (Guillard & Ryther, 1962) under irradiance of 50 μmol photons $\cdot m^{-2} \cdot s^{-1}$ at 18°C and a photoperiod of 16:8 h light:dark. All cultures were transferred to fresh medium every week to ensure that cells remained in their mid-exponential growth phase. Cell size was categorized according to cell diameter. Measurements were conducted using a Nikon Diaphot 300 inverted light microscope (Tokyo, Japan). Image acquisition was obtained with a compact USB camera (ThorCam DCC1545M, ThorLabs, New Jersey, USA), and we calibrated the pixel counter against a hemocytometer grid.

Modeling cell surface CO_2 drawdown

External carbonic anhydrase equilibrates CO_2 and HCO_3^- at the cell surface. Consequently, a good metric for the importance of eCA is the extent of CO_2 drawdown (relative to bulk solution CO_2 concentrations) in the absence and presence of eCA. A model describing the cell surface CO_2 drawdown required to support varying rates of photosynthesis as a function of cell size, with and without eCA, was developed based on previous work by Shen and Hopkinson (2015; assuming spherical cell shapes with a size range of 1–100 μm radius). To calculate net photosynthetic rates (NP), the diatom cellular carbon content (Q_c) versus size relationship of Menden-Deuer and Lessard (2000) was converted from a function of volume to a function of radius (assuming spherical geometry). Next, the growth rate (μ) from Wu, Campbell, et al. (2014; which was derived specifically for centric diatoms) was converted to a function of radius. Finally, using $\mu = NP/Q_c$, a size scaling relationship for NP was derived as: $NP = 0.122 \times R^{2.24}$, where NP is in pmol $\cdot$ cell^{-1} $\cdot$ day^{-1} and R (radius) is in μm. This served as the reference NP rate and various photosynthetic rates were assessed and scaled to this rate (from zero to ×2). We next calculated the contribution of eCA versus no eCA to CO_2 drawdown as a function of cell size. Briefly, Shen and Hopkinson (2015) previously measured eCA activity (expressed as the first order rate constant for eCA-catalyzed CO_2 hydration, k_{sf}) in six centric diatoms (spanning nearly the full range of cell sizes for centric diatoms: equivalent spherical radius 3–67 μm). External carbonic anhydrase activity at low CO_2 (5 μM) was observed to closely follow a power law as a function of the shape radius (R_{shape}), which is used in calculating diffusive fluxes to the cell surface (Marchetti & Cassar, 2009; Pasciak & Gavis, 1975), where $k_{sf} = 6.64 \times 10^{-9} \times (R_{shape})^{2.63}$. The model was solved in Matlab.

Growth rates at four irradiance levels

To determine the optimal growth irradiance for each of the phytoplankton species, we conducted growth experiments at four irradiance levels: 25, 50, 100, and 300 μmol photons $\cdot$ m^{-2} $\cdot$ s^{-1}. Stock cultures of each diatom species were inoculated at low density into aged filtered sterile seawater with f/2 media with 100 μM silicate, in triplicate sterile polystyrene cell culture flasks with vented polyethylene lids. Replicates were positioned on a shelf at varying distances from a white actinic light source (Sylvania ToLEDo 2700 lm 27 W LED Tube Light, Budapest, Hungary) to achieve photon flux densities (PFD) of 25, 50, and 100 μmol $\cdot$ photons $\cdot$ m^{-2} $\cdot$ s^{-1}, measured with a photosynthetically active radiation (PAR) sensor (LI-250 A Light Meter, LI-COR Biosciences, USA). A separate white actinic light source was used to achieve a PFD of 300 μmol photons $\cdot$ m^{-2} $\cdot$ s^{-1} (Kessil A360 X Tuna Sun, California, USA). All growth experiment replicates were maintained at 18°C under a photoperiod of 16:8 h light:dark. The replicates were sampled every 2 days for cell counts,

which were conducted using a Sedgewick Rafter counting chamber (*Coscinodiscus granii* and *Thalassiosira punctigera*) and a Neubauer improved hemocytometer (*Skeletonema dohrnii*). Maximum specific growth rates were calculated using data from the exponential growth portion of the growth curve using the following formula:

$$\mu = \frac{lnX_2 - lnX_1}{t_2 - t_1}$$

where μ is the maximum specific growth rate $\cdot$ day^{-1} and X_1 and X_2 are the cell counts at times t_1 and t_2, respectively.

Effect of eCA inhibition on photosynthetic rates of O_2 evolution in culture populations

We conducted photosynthetic O_2 evolution experiments using 4-mL volume closed oxygen respiration vials (Oxvial4) connected to a Firesting O_2 optical oxygen meter (Pyroscience, Aachen, Germany). A two-point calibration was performed using 0% and 100% air-saturated solutions. Thirty g $\cdot$ L^{-1} sodium dithionite was used to produce a 0% O_2 solution, and an aquarium pump was used to bubble air into H_2O to produce a 100% O_2 solution. Data were recorded using the accompanying O_2 logger software with units of μmol $O_2 \cdot$ L^{-1} selected. We used a combination of blue and white light-emitting diodes (LEDs; Cairn Research, OPTOLED LITE 4141, Kent, UK) as light sources to activate photosynthesis. The LEDs were positioned at opposing angles around the respiration vial at a distance far enough away so as not to raise the internal temperature of the culture sample in the respiration vial. Irradiance intensities were adjusted with an integral controller and measured with a PAR sensor prior to the experiments (LI-250 A Light Meter, LI-COR Biosciences, USA). As this measurement approach requires relatively high biomass, stock cultures for each diatom species (which were maintained under irradiance of 50 μmol photons $\cdot$ m$^{-2} \cdot$ s^{-1}) were inoculated into aged filtered sterile seawater with f/2 media with 100 μM silicate, in five sterile polystyrene cell culture flasks with vented polyethylene lids per species. The five replicates were concentrated and pooled together when the cells were in their exponential growth phase, and three replicate subsamples (each 3 mL) were taken for immediate measurement. We made paired measurements of respiration in the dark followed by photosynthesis-driven [O_2] increase in the light in the presence (control) and absence (eCA inhibition) of eCA at three irradiance intensities (25, 50, and 300 μmol photons $\cdot$ m$^{-2} \cdot$ s^{-1}) during 5-min light:dark cycles. We used 10 μM benzolamide (BZA) to inhibit eCA activity (a member of the sulphonamide class of CA inhibitors). Acetazolamide (AZ) and/or dextran-bound acetazolamide have previously been used as inhibitors in eCA activity studies. Hopkinson et al. (2013) found that 50 μM AZ completely inhibited eCA activity in *Thalassiosira pseudonana* and *T. weissflogii*. We previously showed that 100 μM AZ effectively inhibited the eCA-dependent increase in cell surface pH in *Odontella sinensis* (Chrachri et al., 2018). The same study also determined that inhibiting eCA with 10 μM BZA gave the same reduction in Δ pH change as 100 μM AZ. Previous work has also confirmed that this class of CA inhibitor has no detectable effect on internal CA (iCA) and is therefore not permeable to the plasma membrane (Hopkinson et al., 2013). For the present study, BZA was kindly provided by Dr Juha Voipoi (University of Helsinki), from an original stock synthesized by Dr E.R. Swenson (University of Washington, Seattle, WA, USA).

We performed least-squares regression on the dark respiration phase (decrease in O_2 concentration) and light-driven photosynthetic O_2 evolution O_2 trace data to generate slope values. Gross photosynthetic rates of O_2 evolution were calculated using the formula:

$$O_2 \text{ evolution} = \text{rate of oxygen increase} - \text{dark respiration}$$

Single-cell microelectrode measurements of [O_2], [H^+], and pH

Ion-selective pH microelectrodes were fabricated as previously described (de Beer et al., 2008; Han et al., 2014). Briefly, borosilicate glass capillaries (length 100 mm, outer diameter 1.5 mm, inner diameter 1.17 mm) were pulled to a fine point (outer diameter ~12 μm, inner diameter ~2 μM) using a P-97 micropipette puller (Sutter, Novato, CA, USA). The capillaries were heated at 225°C for 3 h, then salinized by exposure to N,N- dimethyltrimethylsilylamine vapor at 225°C for 1 h. The filling solution was 100 mM NaCl, 20 mM HEPES (pH 7.2), and 10 mM NaOH, and the tip was filled by gentle suction with hydrogen ionophore I—cocktail A (Sigma) containing hydrogen ionophore I (10.0% wt), 2-nitrophenyl octyl ether (89.3% wt), and sodium tetraphenylborate (0.7% wt). The reference electrode was filled with 3 M KCl. Data were recorded using an FD223a amplifier (World Precision Instruments Europe, Hitchin, UK) with pClamp software (Molecular Devices, CA, USA). Each pH microelectrode was calibrated using buffered artificial seawater standards (10 mM HEPES) adjusted to pH 7.0, 8.0, and 9.0 by the addition of HCl or NaOH. The pH_{NBS} in each seawater standard was determined using a Seven Excellence pH meter (Mettler Toledo, Leicester, UK). The slope of the calibrated electrodes ranged from 56 to 59 mV/pH unit (Appendix S1 in the Supporting Information: Figure S1). Oxygen measurements were performed using a Firesting O_2 optode with a tip diameter of 50 μm (Pyroscience, Aachen,

Germany). A two-point calibration was performed using 0% and 100% air-saturated solutions as per the Oxvial4 respiration vials (see above), and data were recorded using the accompanying O_2 logger software in units of $\mu mol\, O_2 \cdot L^{-1}$. Relative rates of photosynthesis were estimated from O_2 measurements using the method of Revsbech et al. (1981), which assumes that for a cell at steady state, the rate of O_2 evolution in the light is equivalent to the initial rate of the decrease in O_2 concentration at the start of the dark period. As the decrease in O_2 represents the combination of O_2 diffusion away from the cell and O_2 uptake by respiratory consumption, our calculation represents gross photosynthetic rate (rather than net). The effect of respiration on the cell surface O_2 concentrations appears to be very small, as previous measurements of cell surface O_2 around other large diatoms (*Odontella sinensis*) in the dark were nearly identical to the bulk seawater (Chrachri et al., 2018). Diatom cells were placed on a glass-bottomed microscopy dish (35 mm diameter) in approximately 2.5 mL of aged and filtered seawater enriched with f/2 media with 100 μM silicate and observed using a Diaphot 300 inverted light microscope (Nikon). The cells were illuminated at 50 and 200 μmol photons $\cdot m^{-2} \cdot s^{-1}$ using a blue LED (Cairn Research, OPTOLED LITE 4141, Kent, UK), which was selected due to rapid photo-bleaching sensitivity of the O_2 optode when exposed to a white light source. (Some preliminary measurements were first made with a white LED to ensure no differences in photosynthetic rates and light-activated O_2/pH elevations were observed between the two light sources.) Measurements were made in a temperature-controlled room (20°C) to ensure constant temperature in the microscopy dish which was periodically monitored with an optical temperature minisensor (TPR430, Pyroscience, Aachen, Germany). The pH microelectrode and O_2 optode were positioned directly against each diatom cell on opposing sides against the silica frustule, using two MP-285 micromanipulators (Sutter, Novato, CA, USA) in order to achieve simultaneous measurements. The cells were perfused with aged and filtered seawater prior to measurements to ensure that carbonate chemistry and dissolved [O_2] were at typical seawater values, and eCA inhibitor treatments were added by perfusion during experiments at a flow rate of approximately 1 mL $\cdot min^{-1}$. A previous similar study predetermined that the microscopy dish did not have a major influence on the formation of the diffusive boundary layer surrounding diatom cells nor on the underlying physiological processes (Chrachri et al., 2018). Microelectrode measurements were performed only on the larger of the three diatom species that were tested in culture population O_2 evolution experiments (*Coscinodiscus granii* and *Thalassiosira punctigera*). This was due to a size mismatch between the smallest diatom, *Skeletonema dohrnii* (9.3 μm diameter) and the tip size of the O_2 optode (50 μm), which was too large to obtain [O_2] measurements at the required spatial resolution for a small cell of this size (Appendix S1: Figure S2).

In addition to single-cell experiments in the presence and absence of eCA under ambient seawater conditions (i.e., pH ~8.1, DIC ~2 mM), we conducted measurements with *Coscinodiscus granii* single cells at lower pH and higher [CO_2]. (See Appendix S1 for methods and inorganic carbon system parameter calculations.) We measured light-activated elevations in [O_2] in two groups of *C. granii* single cells in the presence and absence of eCA in seawater with CO_2 elevated to an estimated value of 52.5 μM (pH 7.65, achieved by bubbling ambient seawater with 100% CO_2 gas): (1) ambient seawater culture (inoculated at pH 8.1) and (2) high CO_2 culture (inoculated at pH 7.65, acclimated for 48 h). We then estimated the extent to which photosynthetic O_2 evolution was inhibited by BZA in single cells at higher [CO_2].

RESULTS

Photosynthetic rate influences diffusive supply of CO_2 to the cell surface

To better understand the potential requirement for eCA during photosynthesis, we employed a cellular model to simulate CO_2 drawdown at the cell surface as a function of photosynthetic rate and cell size. Photosynthetic rates were based on measurements of ^{14}C-DIC incorporation into the biomass of six centric diatoms (equivalent spherical radius 3–67 μm) in the presence and absence of eCA, incubated at 18°C at a light intensity of 200 μmol photons $\cdot m^{-2} \cdot s^{-1}$ (Shen & Hopkinson, 2015). This served as the reference photosynthetic rate ($P_{rel} = 1.0$), and various rates were assessed and scaled to this rate (from zero to x2). In the absence of eCA, the simulation demonstrates that an increase in cell size or relative photosynthetic rate increases the theoretical CO_2 drawdown at the cell surface (indicative of a limiting diffusive supply of CO_2; Figure 2a). For all cell sizes and photosynthetic rates, the CO_2 deficit is effectively abolished by the activity of eCA (Figure 2b). However, in the absence of eCA, the consequences of a change in photosynthetic rate differ significantly with cell size. For a small cell (cell radius of 5 μm, similar to *Skeletonema dohrnii*), the deficit in CO_2 supply at higher photosynthetic rates (P_{rel} 1.5) is only slightly greater than at low photosynthetic rates (P_{rel} 0.5; modeled decrease in cell surface CO_2 is 0.3 μM compared to 0.1 μM). In contrast, for a large cell (50 μm cell radius, similar to *Coscinodiscus granii*), the CO_2 deficit is substantially greater at high photosynthetic rates compared to low photosynthetic rates (decrease in cell surface CO_2 is 10 μM compared to 3 μM). Thus, high photosynthetic

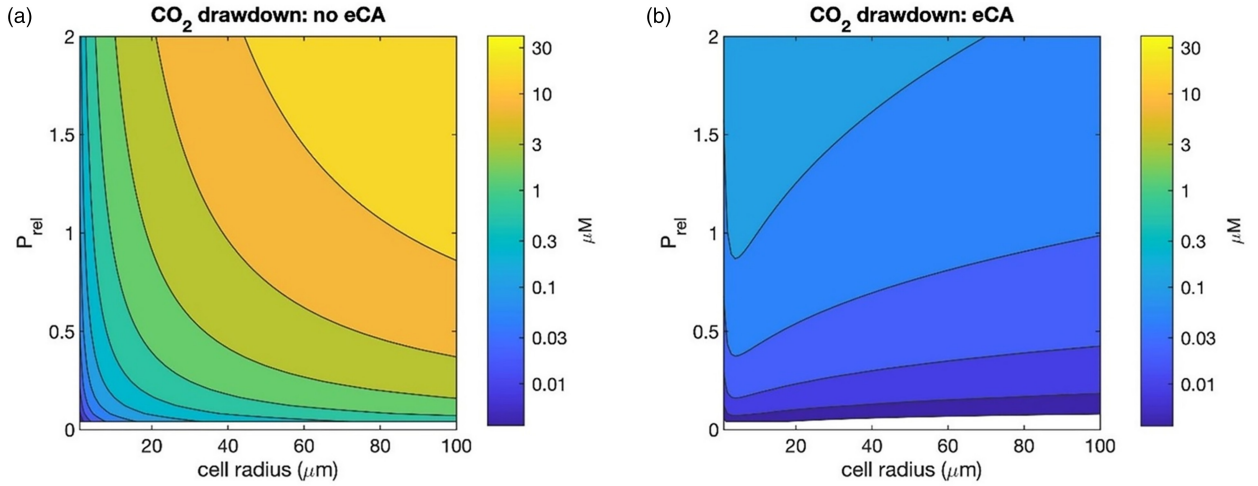

FIGURE 2 Model simulations of cell surface CO_2 drawdown as a function of cell size and photosynthetic rate. (a) Simulation showing the theoretical deficit in CO_2 concentration at the cell surface due to limitation in the diffusive supply of CO_2. In the absence of eCA, CO_2 drawdown increases substantially with photosynthetic rate. The effect is pronounced in large cells, but much less apparent in small cells. Simulations assume a spherical cell. P_{rel} = relative photosynthetic rate. The decrease in CO_2 concentration is shown in μM. (b) In the presence of eCA, which enhanced the catalysis of the equilibrium between HCO_3^- and CO_2, the CO_2 deficit is effectively abolished for all cell sizes at all photosynthetic rates.

rates greatly increase the requirement for eCA in large cells, but the increase in eCA requirement is much less in small cells. The results illustrate the importance of including photosynthetic rates when considering the supply of DIC to the cell surface, as low photosynthetic rates greatly reduce the requirement for eCA, even in very large cells. Photosynthetic rate is, therefore, likely to be a key determinant of the mode of DIC uptake utilized by different species, and we must consider how the CCM operates under optimal conditions for growth, rather than solely at saturating irradiance.

Coscinodiscus granii and *Thalassiosira punctigera* exhibit optimal growth at lower irradiances

We selected three centric diatom species that exhibited a broad range of cell sizes and that were isolated from the same geographical location (station L4, western English Channel). *Coscinodiscus granii* (strain PLY8536), *Thalassiosira punctigera* (strain PLY8538), and *Skeletonema dohrnii* (strain PLY612) exhibited mean cell diameters of 68.8 ± 11.56 μm, 41.1 ± 3.29 μm, and 9.3 ± 0.4 μm respectively (n = 10 cells ± SD). We next established the optimal irradiance for growth, measuring maximum specific growth rates for each species at a range of irradiance levels from 25 to 300 μmol photons · m^{-2} · s^{-1}. Growth rates of the larger species (*C. granii* and *T. punctigera*) were significantly higher at lower irradiances. The maximum specific growth rate (SGR) for *C. granii* was observed at 50 μmol photons · m^{-2} · s^{-1} (mean SGR 0.77 ± 0.06 · d^{-1} compared to 0.55 ± 0.02 at 300 μmol photons · m^{-2} · s^{-1}; see Appendix S1: Figure S3a). Conversely, *S. dohrnii* exhibited higher growth rates at higher irradiance, with the highest growth rates observed at 300 μmol photons · m^{-2} · s^{-1} (1.24 · d^{-1}; see Figure S3c). Among species, *S. dohrnii* exhibited significantly higher growth rates relative to *C. granii* and *T. punctigera* at all light intensities (see Appendix S1: Tables S1 and S2).

The larger species used for our analysis therefore show optimal growth at lower irradiances than the smaller *Skeletonema dohrnii*. As all three diatoms were isolated from the western English Channel, we investigated the irradiance (photosynthetic active radiation, PAR) recorded alongside each observation of these species in the long-term phytoplankton time-series at station L4 between the years 2011 and 2017 (Widdicombe & Harbour, 2021). At the sampling depth of 10 m, PAR associated with all observations of these species was generally low (≤48 μmol photons · m^{-2} · s^{-1}), although it was noticeable that *Skeletonema* sp. were also found at higher irradiances. Ninety-five percent of *Coscinodiscus granii* observations occurred when PAR ≤48 μmol photons · m^{-2} · s^{-1}, whereas 35% of *Skeletonema* sp. observations occurred when PAR ≥48 (up to 378) μmol photons · m^{-2} · s^{-1} (see Appendix S1: Figure S4).

The contribution of eCA to photosynthesis differs with irradiance

We next examined whether the requirement for eCA in each species differed between high and low irradiances. Rates of photosynthetic O_2 evolution were

measured in stirred 3-mL cultures (ambient DIC and pH) at three irradiance levels (25, 50, and 300 μmol photons · m^{-2} · s^{-1}), both in the presence and absence of eCA activity (10 μM BZA). In all three species, photosynthetic rate increased with increasing irradiance, with *Coscinodiscus granii* and *Thalassiosira punctigera* showing a three-fold increase between low and high irradiance. Therefore, short-term increases in irradiance lead to increased rates of photosynthesis in these larger species, although measurements of growth indicate that longer term exposure to high irradiances is not advantageous.

Photosynthetic O_2 evolution by the two larger species exhibited strong sensitivity to the inhibition of eCA, particularly at the highest irradiance. Application of 10 μM BZA to *Coscinodiscus granii* at 300 μmol photons · m^{-2} · s^{-1} significantly decreased O_2 evolution rates by 57% ± 0.89% compared to control cultures (Figure 3a). At lower irradiance levels the extent of inhibition was lessened but was still significantly lower than that of the control cultures (photosynthetic rates decreased by 37% ± 4.9% and 23% ± 5.90% at 50 and 25 μmol photons · m^{-2} · s^{-1}, respectively). Photosynthesis in *Thalassiosira punctigera* was also significantly reduced by the inhibition of eCA at all irradiance levels, although the extent of inhibition did not differ so markedly between low and high irradiance (50% ± 4.26% reduction in photosynthetic O_2 evolution at 300 μmol photons · m^{-2} · s^{-1} compared to 42% ± 9.91% at 25 μmol photons · m^{-2} · s^{-1}) (Figure 3b). In contrast to the larger species, inhibition of eCA did not result in a significant decrease in O_2 evolution in *Skeletonema dohrnii*. A decrease of 19% ± 4.12% was observed at the highest irradiance, but this was not significantly different compared to the untreated control (Figure 3c).

Single-cell measurements of photosynthetic O_2 evolution

Accurate measurements of photosynthetic O_2 evolution using either O_2 electrode or MIMS approaches usually require illumination of a population of cells at high cell density with vigorous stirring. However, many phytoplankton cells are sensitive to mechanical agitation, including large centric diatoms, which may influence the estimation of photosynthetic rate. We, therefore, sought to corroborate our findings using microelectrode approaches to measure photosynthetic rates in single cells in the absence of rapid stirring and high cell densities. We positioned an ion-selective pH microelectrode and an O_2 optode against the frustules of *Coscinodiscus granii* and *Thalassiosira punctigera* to measure O_2 evolution and cell surface pH, which increases substantially during eCA activity (see Appendix S1: Figure S5). We did not include *Skeletonema dohrnii* in these analyses, as we were unable to obtain measurements of O_2 evolution from these much smaller cells using the O_2 optode. Cells were illuminated at low and high irradiance levels (50 and 200 μmol photons · m^{-2} · s^{-1}) for 5 min, separated by 5-min dark phases. At the onset of illumination and at either irradiance level, we observed rapid increases in cell surface [O_2] and pH that were more substantial at the highest irradiance level for both diatoms. For *C. granii*, the mean elevation in cell surface [O_2] at irradiances of 50 and 200 μmol photons · m^{-2} · s^{-1} was 20.13 ± 5.64 and 36.61 ± 7.38 μmol O_2 · L^{-1}, respectively (Figure 4a,b). The rise in cell surface [O_2] was strongly inhibited by the addition of 10 μM BZA, with significant decreases of 33% ± 12% and 54% ± 15% at the low and high irradiance levels, respectively. The increase in cell surface pH was also greatest at

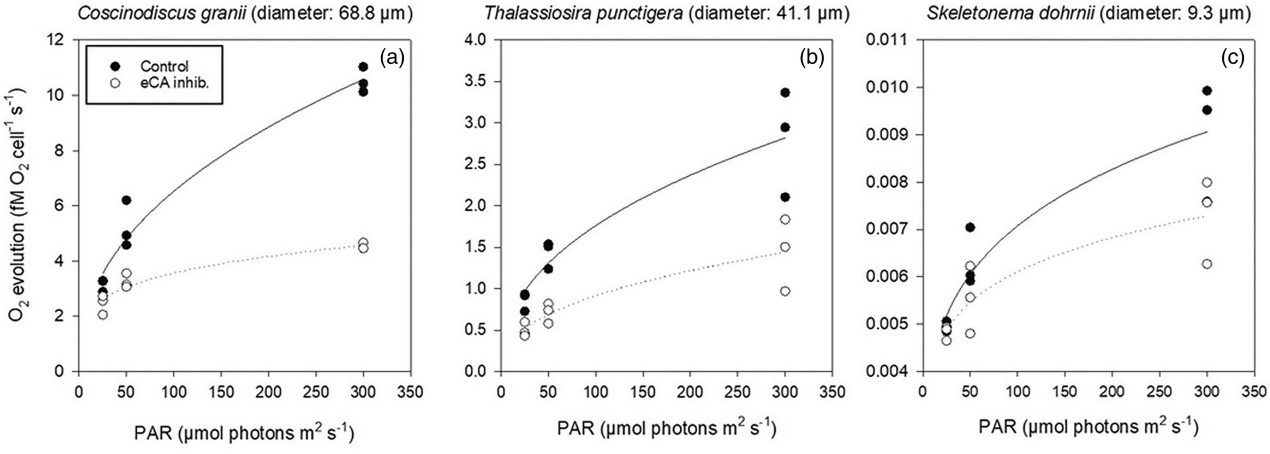

FIGURE 3 The impact of eCA inhibition on photosynthetic O_2 evolution. (a) Rates of photosynthetic O_2 evolution in *Coscinodiscus granii* cultures at three irradiance levels. eCA was inhibited by the addition of 10 uM BZA. Inhibition of eCA resulted in a significant inhibition of photosynthetic O_2 evolution at all irradiances, with the greatest level of inhibition at the highest irradiance level. (b) Inhibition of eCA in *Thalassiosira punctigera* resulted in a significant inhibition of photosynthetic O_2 evolution at all irradiances. (c) Inhibition of eCA in *Skeletonema dohrnii* did not result in a significant inhibition of O_2 evolution at any irradiance. $n = 3$ for all species tested.

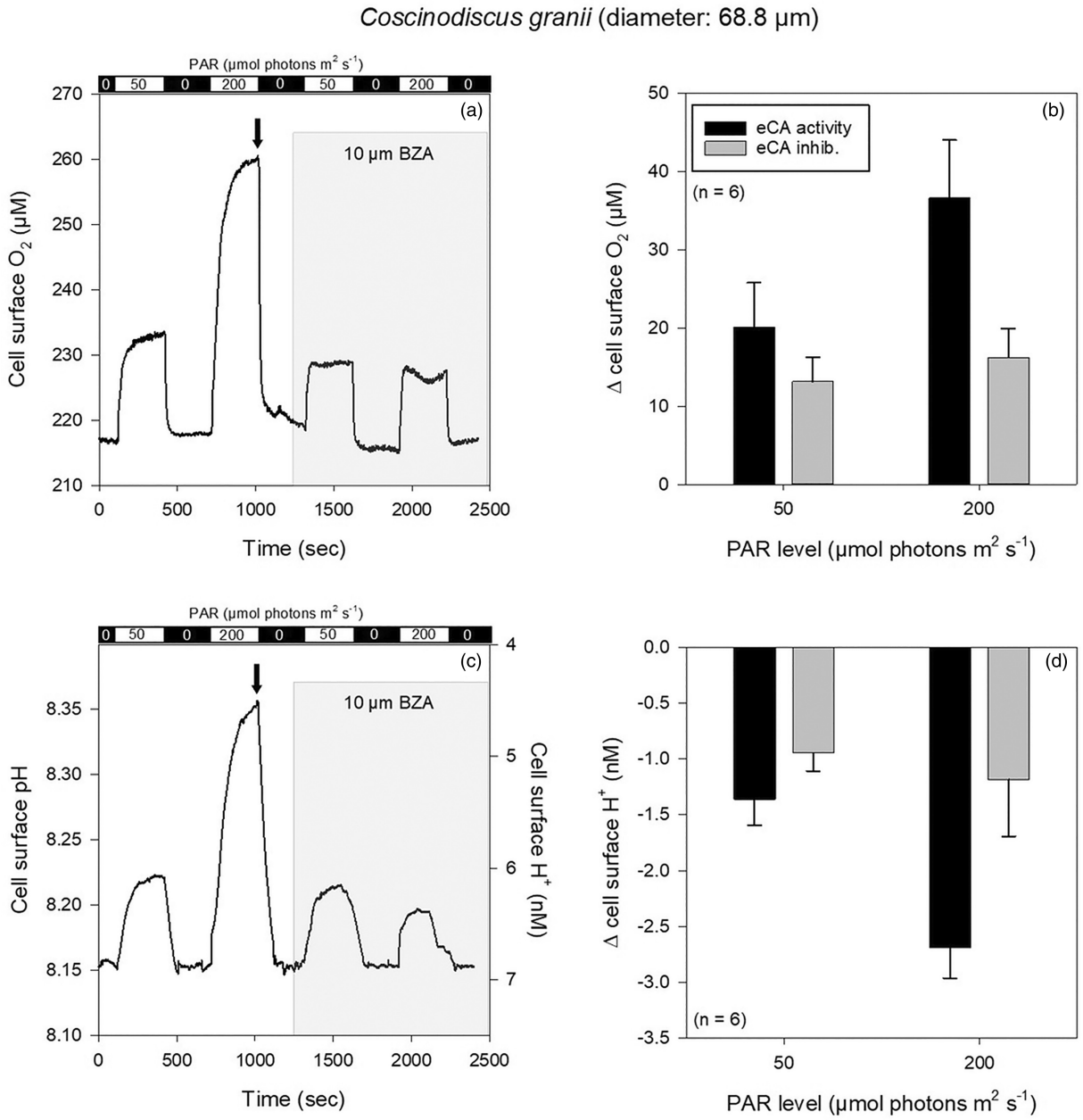

FIGURE 4 Microelectrode measurements of photosynthesis in single *Coscinodiscus granii* cells. (a) Representative trace from a single *C. granii* cell showing cell surface O_2 during alternating light/dark periods. Two different irradiances were applied (50 and 200 µmol photons · m^{-2} · s^{-1}). The shaded area indicates the addition of 10 µM BZA, which has a major impact on photosynthetic O_2 evolution at the higher irradiance. The arrow denotes that O_2 concentration was largely at equilibrium at the maximum rate of photosynthesis. (b) Mean change in the cell surface O_2. Error bars show ± SD. (c) The trace shows microelectrode measurements of cell surface pH from the *C. granii* cell shown in (A). Following illumination, the activity of eCA leads to a substantial rise in cell surface pH, but this increase is reduced in the presence of 10 µM BZA. (d) Mean change in $[H^+]$ at the cell surface. Error bars show ± SD.

the higher irradiance, with a mean decrease in $[H^+]$ of 2.69 ± 0.27 nM (Figure 4c,d). The addition of 10 µM BZA inhibited the decrease in cell surface $[H^+]$ by 30% ± 10% and 56% ± 18% at the low and high irradiance levels, respectively.

For the smaller *Thalassiosira punctigera* cells, light-dependent elevations in cell surface $[O_2]$ were not as substantial as for *Coscinodiscus granii*, with mean increases of 6.84 ± 4.0 and 12.78 ± 5.28 µmol O_2 · L^{-1} at irradiances of 50 and 200 µmol photons · m^{-2} · s^{-1} respectively (Figure 5a,b). When eCA was inhibited, light-activated elevations in $[O_2]$ at the cell surface decreased significantly by 32% ± 15% and 38% ± 9% at the low and high irradiances, respectively. The decrease in cell surface $[H^+]$ was 1.40 ± 0.27 nM at the higher irradiance (Figure 5c,d). 10 µM BZA inhibited the decrease in cell surface $[H^+]$ by 54% ± 11% and 50% ± 18% at the low and high irradiance levels, respectively.

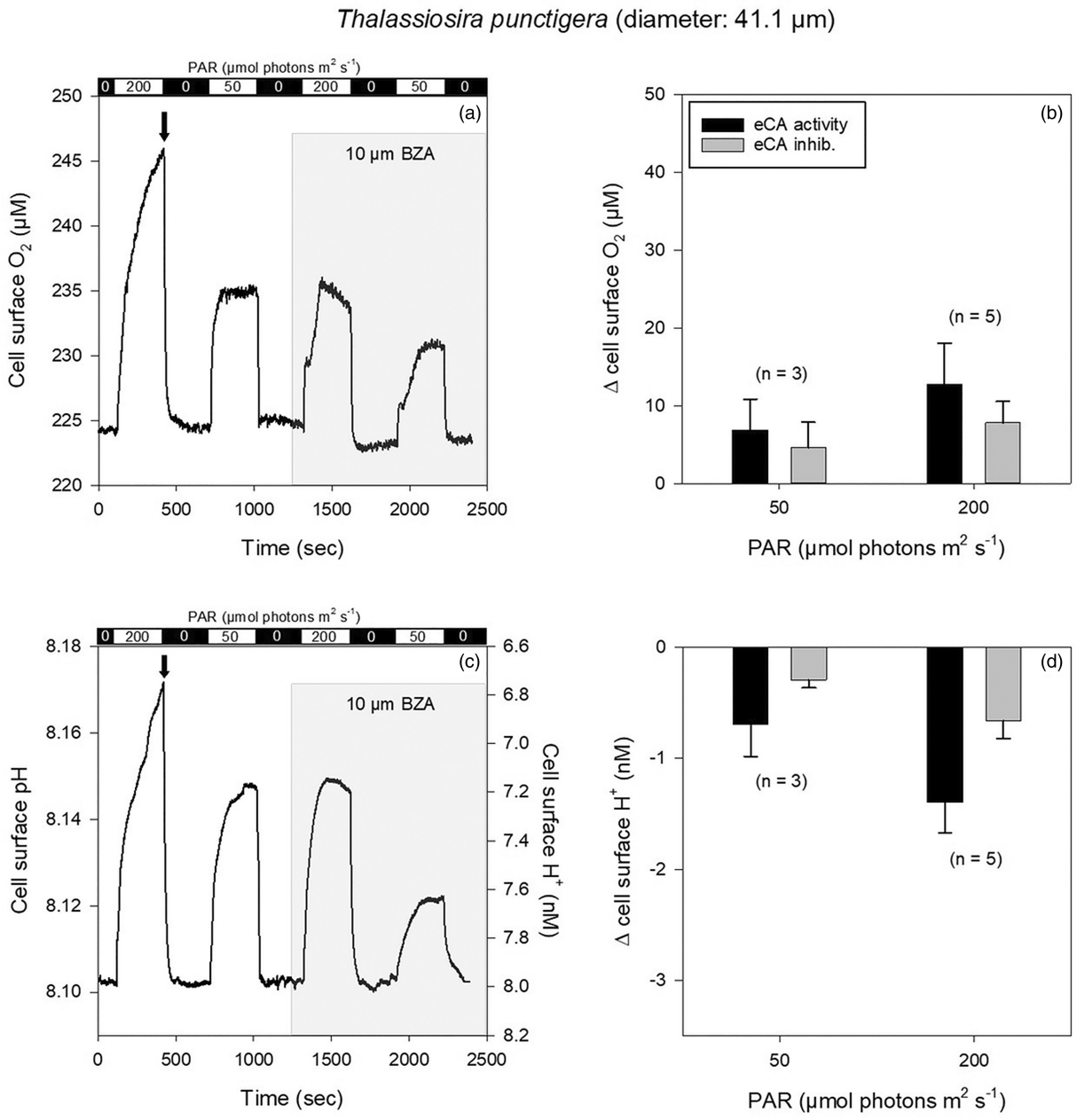

FIGURE 5 Microelectrode measurements of photosynthesis in single *Thalassiosira punctigera* cells. (a) Representative trace from a single *T. punctigera* cell showing cell surface O_2 during alternating light/dark periods. Two different irradiances were applied (50 and 200 µmol photons · m^{-2} · s^{-1}). The shaded area indicates the addition of 10 µM BZA, which has a major impact on photosynthetic O_2 evolution at both irradiances. The arrow denotes cell surface O_2 concentration had not fully reached equilibrium at the higher irradiance in *T. punctigera*, which may have led to an underestimation of the rate of photosynthesis at this irradiance. (b) Mean change in the cell surface O_2. Error bars show ± SD. (c) The trace shows microelectrode measurements of cell surface pH from the *T. punctigera* cell shown in (a). Following illumination, the activity of eCA leads to a substantial rise in cell surface pH, but this increase is reduced in the presence of 10 µM BZA. (d) Mean change in [H^+] at the cell surface. Error bars show ± SD.

The steady-state concentration of O_2 at the surface of a photosynthesizing cell is determined by the combination of the rate of photosynthetic O_2 evolution and the rate at which O_2 diffuses away from the cell. When the light is turned off, the instantaneous rate of the decrease in O_2 is a measure of the rate at which O_2 diffuses away from the cell, which is equivalent to the rate of photosynthetic O_2 evolution if these processes have reached equilibrium (Revsbech et al., 1981). We therefore estimated the extent to which photosynthetic O_2 evolution was inhibited by BZA in each species at the different irradiances. We observed a 26% ± 2.95% decrease in photosynthetic rates in *Coscinodiscus granii* at 50 µmol photons · m^{-2} · s^{-1} when eCA was inhibited, while at 200 µmol photons · m^{-2} · s^{-1} photosynthetic rates decreased by 53% ± 4.7% (Figure 6a). For *Thalassiosira punctigera*, photosynthetic rates declined by 30% ± 4.9% at 50 µmol photons · m^{-2} · s^{-1} and

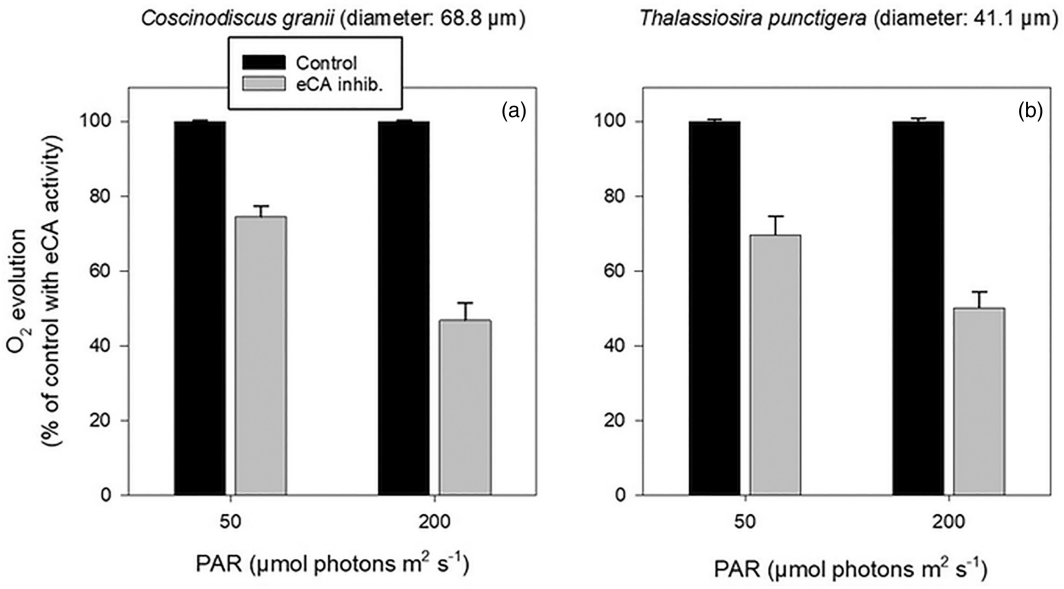

FIGURE 6 Rates of photosynthetic O_2 evolution calculated from microelectrode measurements. (a) Mean rates of photosynthetic O_2 evolution in *Coscinodiscus granii* estimated from single-cell microelectrode measurements. Data are shown relative to the untreated control (eCA present) and following perfusion with 10 µM BZA (eCA inhibition) at two irradiances. $n = 6$ cells. (b) Measurements as in (a) but in *Thalassiosira punctigera* cells. $n = 3$ and 5 cells for 50 and 200 µmol photons · m^{-2} · s^{-1}, respectively.

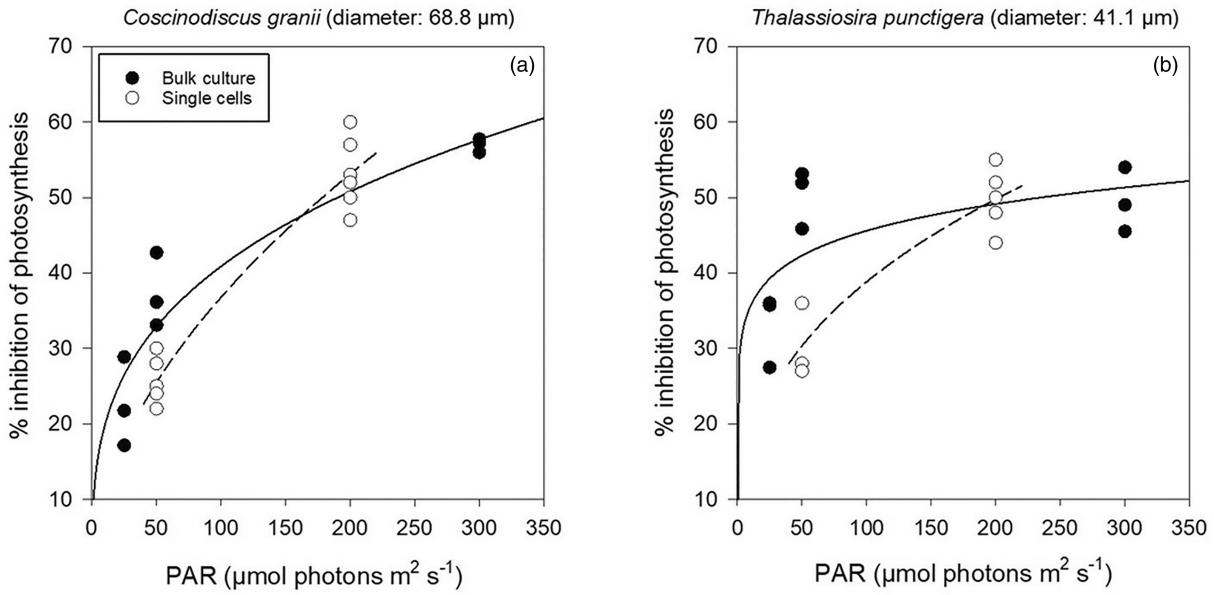

FIGURE 7 Comparison of the contribution of eCA to photosynthesis measured by different techniques. (a) Inhibition in the rate of photosynthetic O_2 evolution in *Coscinodiscus granii* caused by the application of eCA inhibitors (10 µM BZA). Data from cultures (3-mL vial) are compared with microelectrode measurements of single cells. (b) As in (a) but for *Thalassiosira punctigera*.

by 50% ± 4.15% at 200 µmol photons · m^{-2} · s^{-1} when eCA was inhibited (Figure 6b). Thus, eCA contributes significantly to photosynthetic O_2 evolution in both diatoms at both irradiances.

Overall, the results from single cells agree broadly from those obtained at the population level (Figure 7), indicating that the single-cell measurements are a reliable measurement of photosynthetic activity and that these large diatoms are not too adversely affected by the stirring and high cell densities required for the population level measurements. Direct comparisons between the two techniques are hampered by difficulties in replicating the irradiances experienced by individual cells within the different experimental vessels, which may have contributed to the apparent discrepancy between *Thalassiosira punctigera* cultures and single cells at 50 µmol photons · m^{-2} · s^{-1}. Nevertheless, there is a broad trend of an increased

contribution of eCA to photosynthesis at higher photosynthetic rates (See Appendix S1: Figure S6). This effect is most pronounced in the larger species, although it should be noted that only a relatively small range of species and cell sizes were examined in this study.

We measured O_2 evolution in two groups of *Coscinodiscus granii* single cells exposed to lower pH and higher CO_2 (pH 7.65, 52.5 μM CO_2 estimated, 2.25 mM total DIC estimated): 1) cells from an ambient seawater culture (inoculated at pH 8.1) and 2) cells from a high CO_2 culture (inoculated at pH 7.65, acclimated for 48 h). At the onset of illumination (200 μmol photons · m^{-2} · s^{-1}), we observed similar rapid increases in cell surface [O_2] compared to our measurements in ambient seawater with typical DIC values (pH 8.1, 2 mM DIC). However, upon application of 20 μM BZA, the rise in cell surface [O_2] was only weakly inhibited, with decreases of 7.6% ± 4% for cells from the ambient seawater culture and 11.9% ± 9% for cells pre-acclimated to high CO_2 seawater (See Appendix S1: Figure S7a,b). Similarly, photosynthetic O_2 evolution was only weakly inhibited by 20 μM BZA. Photosynthetic rates decreased by 6% ± 10% in *C. granii* single cells from the ambient seawater culture and by 5.7% ± 5.9% in cells pre-acclimated to elevated CO_2 (See Figure S7c).

DISCUSSION

Our cellular modeling shows that for small cells the deficit between diffusive CO_2 supply and demand is relatively low, even at high photosynthetic rates. In contrast, photosynthetic rates have a major impact on diffusive CO_2 supply to large cells. It is well established that the boundary layer will influence CO_2 diffusion to a large cell (Wolf-Gladrow 1997), but our results demonstrate that we must also consider this in the context of DIC demand. Although we only examined three species, our experimental data largely support our modeling study, illustrating that eCA contributes to photosynthesis in the two large centric diatoms at ambient pH and DIC, whereas it did not make a significant contribution to photosynthesis in the much smaller *Skeletonema dohrnii* cells. Moreover, *Coscinodiscus granii* exhibited a greater reliance on eCA to support higher photosynthetic rates at increased irradiances, suggesting that the deficit in diffusive CO_2 supply was met primarily by eCA. As this effect was observed in single cells within a short time period (minutes), our results demonstrate how eCA can be used by *C. granii* to rapidly modulate DIC uptake following changes in DIC demand. A similar effect was also apparent in *Thalassiosira punctigera*, although the increase in the contribution of eCA at the higher irradiances was much smaller.

Although our results indicate a substantial requirement for eCA in two large diatom species, several previous studies did not identified a clear relationship between cell size and eCA activity in diatoms. No correlation was seen between eCA activity and surface area to cell volume ratio in a survey of 17 diverse diatom species (Martin & Tortell, 2008). Examination of six centric diatoms with a cell radius between 3 and 67 μm showed that eCA activity does increase with cell size, although inhibiting eCA revealed no overall relationship between cell size and the extent of inhibition of photosynthesis (Shen & Hopkinson, 2015). Moreover, this study only identified a significant decrease in photosynthetic rate of *Thalassiosira punctigera* and *Coscinodiscus wailesii* due to inhibition of eCA at low CO_2 conditions (0.5 mM DIC, pH = 8.4, CO_2 1.2 μM) and not at ambient DIC (2 mM DIC, pH 8.2, CO_2 8.5 μM; Shen & Hopkinson, 2015). This contrasts with our results but may relate to the different techniques used to assess photosynthesis (carbon fixation vs. O_2 evolution).

Under ambient DIC conditions, we did not observe a substantial contribution of eCA to photosynthesis in *Skeletonema dohrnii*, although it is likely that eCA is used by smaller diatoms under conditions where DIC becomes depleted. Nimer et al. (1998) observed light-dependent activation of eCA in *S. costatum* at an irradiance of 100 μmol photons · m^{-2} · s^{-1}, but only when CO_2 was less than 5 μM. Further work on *S. costatum* showed that eCA was detectable by light activation in cell cultures grown at 4 μM CO_2 but not at 12 and 31 μM CO_2, with a 2.5-fold increase in eCA activity observed at an irradiance of 210 compared to 30 μmol photons · m^{-2} · s^{-1} (Chen & Gao, 2003). This further demonstrates the effect of irradiance on DIC demand, even in small diatoms. Other work on smaller diatoms also reported that eCA inhibition reduced photosynthetic rates only at low CO_2 concentrations and not at typical seawater values in the diatoms *Thalassiosira pseudonana*, *T. weissflogii*, and *S. costatum* (Burkhardt et al., 2001; Hopkinson et al., 2013; Rost et al., 2003).

Diatoms use multiple strategies to overcome the diffusive supply of CO_2 to the cell surface (Tsuji et al., 2017), with different species increasing either eCA activity or direct HCO_3^- uptake when diffusive CO_2 supply becomes limiting (Burkhardt et al., 2001; Martin & Tortell, 2006; Trimborn et al., 2008). It is important to note that our study has only examined whether the requirement for eCA differs in response to a change in DIC demand, and we have not examined whether there is also a change in the proportion of DIC taken up as HCO_3^-. Although the application of inhibitors to assess the contribution of eCA to diatom photosynthesis has been used extensively (Burkhardt et al., 2001; Elzenga et al., 2000; Iglesias-Rodriguez & Merrett, 1997; Martin & Tortell, 2008; Moroney et al., 1985; Nimer et al., 1998; Rost et al., 2003),

this approach is subject to a number of key assumptions. The first of these relates to the specificity of the inhibitor and its site of action. Acetazolamide and benzolamide are assumed to act only on extracellular CAs as they are poorly membrane-permeable. Hopkinson et al. (2013) observed no detectable inhibition of intracellular CAs by AZ or DBAZ in *Thalassiosira pseudonana* or *T. weissflogii* in short-term studies, supporting this assumption. Another critical assumption is that the reduction in photosynthetic rate caused by eCA inhibition is a direct measure of the contribution of eCA to total DIC uptake. This approach requires that inhibition of eCA has no impact on the other mechanisms of DIC uptake, i.e., that an alternative mechanism such as direct HCO_3^- uptake is not activated in order to compensate for the lack of eCA activity. Our previous study using pH and CO_3^{2-} microelectrodes in the large diatom *Odontella sinensis* provided some evidence to suggest that direct HCO_3^- uptake was stimulated following inhibition of eCA (Chrachri et al., 2018). If this is the case in other species, then many studies that rely on eCA inhibition (including the current study) may have underestimated the contribution of eCA to photosynthetic DIC uptake.

Variability in response, requirement for rapid modulation

Diatoms exist in diverse and highly variable environments where significant variability in DIC supply and demand may be imposed by fluctuations in irradiance, temperature, nutrient supply, and carbonate chemistry of natural seawater (Broekhuizen et al., 1998; Kitidis et al., 2012; Macintyre et al., 2000). However, many of these parameters change relatively slowly, over timescales of hours to days. For example, changes in nutrient loads typically occur over relatively longer periods (days to seasons) in many marine systems (Holmes et al., 1989). Likewise, due to seawater's capacity for high levels of latent heat, temperature variations in surface oceans occur primarily on daily to seasonal timescales (Roberts et al., 2016). The concentration of CO_2 in seawater can also fluctuate, driven by seasonal changes due to physical processes or changes over shorter timescales due to biotic influences, such as CO_2 drawdown during a phytoplankton bloom. Carbon dioxide concentrations in productive coastal waters can range between 30 and 6 μM (Kitidis et al., 2012; Kranz et al., 2015), so enhanced eCA activity may be particularly important at the end of phytoplankton blooms when CO_2 concentrations can be significantly reduced below typical concentrations. Diatoms can respond to changes in CO_2 availability over these timescales by increasing their ability to utilize HCO_3^-, via increased eCA activity and/or increased direct HCO_3^- uptake (Iglesias-Rodriguez & Merrett, 1997; Rost et al., 2003). However, diatom cells must also respond to changes in DIC demand over much shorter timescales. Phytoplankton are subjected to rapid changes in both the intensity and spectral quality of light within minutes, seconds, or even milliseconds (Schubert & Forster, 1997). Changes in irradiance will have a near-instant effects on rates of photosynthetic electron transport and the demand for DIC to support carbon fixation. There remains very little understanding of how the activity of the CCM responds to changes in photosynthetic rates on these timescales. The magnitude and frequency of the changes in irradiance encountered by phytoplankton cells in the surface ocean, particularly in areas of turbulent mixing or with intermittent cloud cover, suggests that an ability to modulate DIC uptake on these timescales is a primary requirement of the diatom CCM.

Both of the larger diatoms in our study, *Coscinodiscus granii* and *Thalassiosira punctigera*, appeared to be better suited to conditions of low irradiance, exhibiting optimal growth rates at 50 $\mu mol\,photons \cdot m^{-2} \cdot s^{-1}$. This corresponds with observations from the station L4 time series, where both these species are predominately found at low irradiances. In their natural environment (i.e., standard seawater carbonate chemistry and low irradiance), the requirement for eCA will be relatively low in both species due to the lower rates of photosynthesis. However, the presence of eCA in these cells ensures that the CO_2 concentration at the cell surface does not become depleted, even if photosynthetic rate and consequently DIC demand rapidly increase, due to increased irradiance. Thus, eCA can be utilized dynamically to meet the increased demands for DIC uptake and prevent the limitation of DIC supply (Yan et al., 2018).

Larger cell sizes in diatoms are associated with lower maximum growth rates (when determined for nutrient-replete cultures at a given irradiance level; Geider et al., 1986). This has been attributed to a reduced ability of large diatoms to harvest light efficiently, due in part to the self-shading of pigments in large cells (the package effect), which leads to a lower photosynthetic rate per unit chlorophyll (Finkel, 2001; Geider et al., 1986). However, energetic costs associated with DIC uptake may also contribute to lower maximum growth rates at high irradiances, as these would be much greater in larger cells. Interestingly, the proportion of total cellular nitrogen attributed to RuBisCO for CO_2 fixation is also much greater in large diatoms, which may relate to differences in the supply of CO_2 to RuBisCO in larger cells (Wu, Campbell, et al., 2014). The combination of these factors may mean that large diatoms are better suited to lower irradiances. For example, a small number of non-CCM macroalgal species exhibit exclusive CO_2 diffusive uptake (Raven et al., 1995) with a corresponding low

light spatial distribution in deep habitats or beneath dense canopies where carbon demands of individuals are lower (Cornwall et al., 2015; Hepburn et al., 2011; Lovelock et al., 2020).

Elevated CO_2

Ongoing increases in seawater CO_2 concentrations are likely to become a feature of future oceans, though cellular model simulations have indicated that eCA will still be required by large diatoms even at elevated CO_2, albeit at a lower level of activity (Chrachri et al., 2018). We confirmed this experimentally, with observations (in the absence of eCA) of a marked decrease in the level of inhibition of light-activated elevations in $[O_2]$ and photosynthetic rates in *Coscinodiscus granii* single cells when CO_2 was elevated. Increasing CO_2 in the inorganic carbon system clearly resulted in restoring affinity for CO_2 in the absence of eCA, though a low requirement for eCA was evident. This may lead to reduced energy demands on eCA resulting in resource allocation to other cellular processes such as growth. Observations of growth responses in a range of diatoms under elevated CO_2 showed a growth enhancement of ~5% in small centric diatoms (*Thalassiosira pseudonana*, *T. guillardii*, and *T. weissflogii*), while growth rates increased by ~30% in the larger *T. punctigera* and *C. wailesii* (Wu, Campbell, et al., 2014). Additionally, a recent modeling study has suggested that intermediate-size diatoms might benefit the most from CO_2 enrichment, as the CO_2 supply to small cells is not limiting under ambient CO_2 whereas larger cells utilize a larger proportion of HCO_3^- uptake and, therefore, will not benefit as much from increased CO_2 concentrations (Zhang & Luo, 2022). This model also considers how the energetic cost of direct HCO_3^- uptake may lead to lower growth rates in larger cells, but the interpretation of these findings is complex, and it is clear that a greater understanding of the operation of the diatom CCM is necessary before we can accurately model the response of individual species and communities to changes in seawater CO_2. Notably, a synthesis of the effect of CO_2 enrichment on natural diatom communities demonstrated a shift to larger cell sizes in 12 out of 13 experiments in which cell size was reported, indicating that large cells respond positively to short-term CO_2 addition (Bach & Taucher, 2019).

Summary

Our data support a role for eCA in enhancing the supply of CO_2 to the cell surface by rapidly catalyzing the conversion of HCO_3^- to CO_2. We observed a trend of increasing inhibition of photosynthesis with increasing cell size and photosynthetic rate in the absence of eCA among three diatoms of contrasting size, which supports the findings of our cellular model. Together, our data indicate that the requirement for eCA is strongly driven by changes in DIC demand, which has important implications for future studies comparing the operation of the diatom CCM among species or at different seawater carbonate chemistries.

AUTHOR CONTRIBUTIONS

Matthew Keys: Conceptualization (equal); data curation (lead); formal analysis (lead); investigation (equal); methodology (equal); project administration (supporting); writing – original draft (lead); writing – review and editing (equal). **Andrea Highfield:** Writing – review and editing (supporting). **Brian Hopkinson:** Methodology (lead); software (lead). **Abdul Chrachri:** Methodology (supporting). **Colin Brownlee:** Writing – review and editing (supporting). **Glen Wheeler:** Conceptualization (lead); funding acquisition (lead); investigation (lead); methodology (lead); project administration (lead); resources (lead); supervision (lead); writing – original draft (supporting); writing – review and editing (supporting).

ACKNOWLEDGMENTS

This work was supported by funding from The Natural Environment Research Council (NERC), Grant Reference NE/T000848/1.

DATA AVAILABILITY STATEMENT

The relevant data from this study are available from the authors.

ORCID

Matthew Keys https://orcid.org/0009-0004-7609-3407
Brian Hopkinson https://orcid.org/0000-0002-0844-0794
Glen L. Wheeler https://orcid.org/0000-0002-4657-1701

REFERENCES

Armbrust, E. V. (2009). The life of diatoms in the world's oceans. *Nature*, *459*(7244), 185–192. https://doi.org/10.1038/nature08057

Bach, T. L., & Taucher, J. (2019). CO_2 effects on diatoms: A synthesis of more than a decade of ocean acidification experiments with natural communities. *Ocean Science*, *15*(4), 1159–1175. https://doi.org/10.5194/os-15-1159-2019

Broekhuizen, N., Hadfield, M., & Taylor, A. (1998). Seasonal photoadaptation and diatom dynamics in temperate waters. *Marine Ecology Progress Series*, *175*, 227–239.

Burkhardt, S., Amoroso, G., Riebesell, U., & Sültemeyer, D. (2001). CO_2 and HCO_3^- uptake in marine diatoms acclimated to different CO_2 concentrations. *Limnology and Oceanography*, *46*(6), 1378–1391. https://doi.org/10.4319/lo.2001.46.6.1378

Chen, X., & Gao, K. (2003). Effect of CO_2 concentrations on the activity of photosynthetic CO_2 fixation and extracelluar carbonic anhydrase in the marine diatom *Skeletonema costatum*. *Chinese Science Bulletin*, *48*(23), 2616–2620. https://doi.org/10.1360/03wc0084

Chrachri, A., Hopkinson, B. M., Flynn, K., Brownlee, C., & Wheeler, G. L. (2018). Dynamic changes in carbonate chemistry in the microenvironment around single marine phytoplankton cells. *Nature Communications*, *9*(1), 1–12. https://doi.org/10.1038/s41467-017-02426-y

Cornwall, C. E., Revill, A. T., & Hurd, C. L. (2015). High prevalence of diffusive uptake of CO_2 by macroalgae in a temperate subtidal ecosystem. *Photosynthesis Research*, *124*(2), 181–190. https://doi.org/10.1007/s11120-015-0114-0

de Beer, D., Bissett, A., de Wit, R., Jonkers, H., Köhler-Rink, S., Nam, H., Kim, B. H., Eickert, G., & Grinstain, M. (2008). A microsensor for carbonate ions suitable for microprofiling in freshwater and saline environments. *Limnology and Oceanography: Methods*, *6*(10), 532–541. https://doi.org/10.4319/lom.2008.6.532

de Beer, D., & Larkum, A. W. D. (2001). Photosynthesis and calcification in the calcifying algae *Halimeda discoidea* studied with microsensors. *Plant, Cell and Environment*, *24*(11), 1209–1217. https://doi.org/10.1046/j.1365-3040.2001.00772.x

Elzenga, J. T. M., Prins, H. B. A., & Stefels, J. (2000). The role of extracellular carbonic anhydrase activity in inorganic carbon utilization of *Phaeocystis globosa* (Prymnesiophyceae): A comparison with other marine algae using the isotopic disequilibrium technique. *Limnology and Oceanography*, *45*(2), 372–380. https://doi.org/10.4319/lo.2000.45.2.0372

Falkowski, P. G., Katz, M. E., Knoll, A. H., Quigg, A., Raven, J. A., Schofield, O., & Taylor, F. J. R. (2004). The evolution of modern eukaryotic phytoplankton. *Science*, *305*(5682), 354–360. https://doi.org/10.1126/science.1095964

Finkel, Z. V. (2001). Light absorption and size scaling of light-limited metabolism in marine diatoms. *Limnology and Oceanography*, *46*(1), 86–94. https://doi.org/10.4319/lo.2001.46.1.0086

Finkel, Z. V., Vaillancourt, C. J., Irwin, A. J., Reavie, E. D., & Smol, J. P. (2009). Environmental control of diatom community size structure varies across aquatic ecosystems. *Proceedings of the Royal Society B: Biological Sciences*, *276*(1662), 1627–1634. https://doi.org/10.1098/rspb.2008.1610

Gavis, J., & Ferguson, J. F. (1975). Kinetics of carbon dioxide uptake by phytoplankton at high pH. *Limnology and Oceanography*, *20*(2), 211–221. https://doi.org/10.4319/lo.1975.20.2.0211

Geider, R., Piatt, T., & Raven, J. (1986). Size dependence of growth and photosynthesis in diatoms: A synthesis. *Marine Ecology Progress Series*, *30*, 93–104. https://doi.org/10.3354/meps030093

Guillard, R. R. L., & Ryther, J. H. (1962). Studies of marine planktonic diatoms: I. *Cyclotella nana* Husedt, and Detonula Confervacea (Cleve) gran. *Canadian Journal of Microbiology*, *8*, 229–239.

Han, C., Cai, W. J., Wang, Y., & Ye, Y. (2014). Calibration and evaluation of a carbonate microsensor for studies of the marine inorganic carbon system. *Journal of Oceanography*, *70*(5), 425–433. https://doi.org/10.1007/s10872-014-0243-7

Hepburn, C. D., Pritchard, D. W., Cornwall, C. E., Mcleod, R. J., Beardall, J., Raven, J. A., & Hurd, C. L. (2011). Diversity of carbon use strategies in a kelp forest community: Implications for a high CO_2 ocean. *Global Change Biology*, *17*(7), 2488–2497. https://doi.org/10.1111/j.1365-2486.2011.02411.x

Holmes, J. J., Weger, H. G., & Turpin, D. H. (1989). Chlorophyll a fluorescence predicts Total photosynthetic electron flow to CO_2 or NO_3^-/NO_2^- under transient conditions. *Plant Physiology*, *91*(1), 331–337. https://doi.org/10.1104/pp.91.1.331

Hopkinson, B. M., Dupont, C. L., & Matsuda, Y. (2016). The physiology and genetics of CO_2 concentrating mechanisms in model diatoms. *Current Opinion in Plant Biology*, *31*, 51–57. https://doi.org/10.1016/j.pbi.2016.03.013

Hopkinson, B. M., Meile, C., & Shen, C. (2013). Quantification of extracellular carbonic anhydrase activity in two marine diatoms and investigation of its role. *Plant Physiology*, *162*(2), 1142–1152. https://doi.org/10.1104/pp.113.217737

Hurd, C. L., Cornwall, C. E., Currie, K., Hepburn, C. D., McGraw, C. M., Hunter, K. A., & Boyd, P. W. (2011). Metabolically induced pH fluctuations by some coastal calcifiers exceed projected 22nd century ocean acidification: A mechanism for differential susceptibility? *Global Change Biology*, *17*(10), 3254–3262. https://doi.org/10.1111/j.1365-2486.2011.02473.x

Iglesias-Rodriguez, M. D., & Merrett, M. J. (1997). Dissolved inorganic carbon utilization and the development of extracellular carbonic anhydrase by the marine diatom *Phaeodactylum tricornutum*. *New Phytologist*, *135*(1), 163–168. https://doi.org/10.1046/j.1469-8137.1997.00625.x

John-Mckay, M. E., & Colman, B. (1997). Note variation in the occurrence of external carbonic anhydrase among strains of the marine diatom *Phaeodactylum Tricornutum* (Bacillariphyceae). *Journal of Phycology*, *33*, 988–990.

Kitidis, V., Hardman-Mountford, N. J., Litt, E., Brown, I., Cummings, D., Hartman, S., Hydes, D., Fishwick, J. R., Harris, C., Martinez-Vicente, V., Woodward, E. M. S., & Smyth, T. J. (2012). Seasonal dynamics of the carbonate system in the Western English Channel. *Continental Shelf Research*, *42*, 30–40. https://doi.org/10.1016/j.csr.2012.04.012

Kranz, S. A., Young, J. N., Hopkinson, B. M., Goldman, J. A. L., Tortell, P. D., & Morel, F. M. M. (2015). Low temperature reduces the energetic requirement for the CO_2 concentrating mechanism in diatoms. *New Phytologist*, *205*(1), 192–201. https://doi.org/10.1111/nph.12976

Kühn, S. F., & Raven, J. A. (2008). Photosynthetic oscillation in individual cells of the marine diatom *Coscinodiscus wailesii* (Bacillariophyceae) revealed by microsensor measurements. *Photosynthesis Research*, *95*(1), 37–44. https://doi.org/10.1007/s11120-007-9221-x

Liu, F., Gledhill, M., Tan, Q.-G., Zhu, K., Zhang, Q., Salaun, P., Tagliabue, A., Zhang, Y., Weiss, D., Achterberg, E. P., & Korchev, Y. (2022). The phycosphere pH of unicellular nano- and micro- phytoplankton cells and consequences for iron speciation. *The ISME Journal*, *16*, 2329–2336. https://doi.org/10.1038/s41396-022-01280-1

Lovelock, C. E., Reef, R., Raven, J. A., & Pandolfi, J. M. (2020). Regional variation in $\delta 13^C$ of coral reef macroalgae. *Limnology and Oceanography*, *65*(10), 2291–2302. https://doi.org/10.1002/lno.11453

Macintyre, H. L., Kana, T. M., & Geider, R. J. (2000). The effect of water motion on short-term rates of photosynthesis by marine phytoplankton. *Trends in Plant Science*, *5*(1), 12–17.

Malerba, M. E., Marshall, D. J., Palacios, M. M., Raven, J. A., & Beardall, J. (2021). Cell size influences inorganic carbon acquisition in artificially selected phytoplankton. *New Phytologist*, *229*(5), 2647–2659. https://doi.org/10.1111/nph.17068

Marchetti, A., & Cassar, N. (2009). Diatom elemental and morphological changes in response to iron limitation: A brief review with potential paleoceanographic applications. *Geobiology*, *7*(4), 419–431. https://doi.org/10.1111/j.1472-4669.2009.00207.x

Martin, C. L., & Tortell, P. D. (2006). Bicarbonate transport and extracellular carbonic anhydrase activity in Bering Sea phytoplankton assemblages: Results from isotope disequilibrium experiments. *Limnology and Oceanography*, *51*(5), 2111–2121. https://doi.org/10.4319/lo.2006.51.5.2111

Martin, C. L., & Tortell, P. D. (2008). Bicarbonate transport and extracellular carbonic anhydrase in marine diatoms. *Physiologia Plantarum*, *133*(1), 106–116. https://doi.org/10.1111/j.1399-3054.2008.01054.x

Menden-Deuer, S., & Lessard, E. J. (2000). Carbon to volume relationships for dinoflagellates, diatoms, and other protist plankton.

Limnology and Oceanography, *45*(3), 569–579. https://doi.org/10.4319/lo.2000.45.3.0569

Milligan, A. J., Mioni, C. E., & Morel, F. M. M. (2009). Response of cell surface pH to pCO_2 and iron limitation in the marine diatom *Thalassiosira weissflogii*. *Marine Chemistry*, *114*(1–2), 31–36. https://doi.org/10.1016/j.marchem.2009.03.003

Mitchell, B. G., Brody, E. A., Holm-Hansen, O., McClain, C., & Bishop, J. (1991). Light limitation of phytoplankton biomass and macronutrient utilization in the Southern Ocean. *Limnology and Oceanography*, *36*(8), 1662–1677. https://doi.org/10.4319/lo.1991.36.8.1662

Moroney, J. V., Husic, H. D., & Tolbert, N. E. (1985). Effect of carbonic anhydrase inhibitors on inorganic carbon accumulation by *Chlamydomonas reinhardtii*. *Plant Physiology*, *79*(1), 177–183. https://doi.org/10.1104/pp.79.1.177

Nakajima, K., Tanaka, A., & Matsuda, Y. (2013). SLC4 family transporters in a marine diatom directly pump bicarbonate from seawater. *Proceedings of the National Academy of Sciences of the United States of America*, *110*(5), 1767–1772. https://doi.org/10.1073/pnas.1216234110

Nelson, D. M., Tréguer, P., Brzezinski, M. A., Leynaert, A., & Quéguiner, B. (1995). Production and dissolution of biogenic silica in the ocean: Revised global estimates, comparison with regional data and relationship to biogenic sedimentation. *Global Biogeochemical Cycles*, *9*(3), 359–372. https://doi.org/10.1029/95GB01070

Nimer, N. A., Brownlee, C., & Merrett, M. J. (1999). Extracellular carbonic anhydrase facilitates carbon dioxide availability for photosynthesis in the marine dinoflagellate *Prorocentrum micans*. *Plant Physiology*, *120*(1), 105–111. https://doi.org/10.1104/pp.120.1.105

Nimer, N. A., Guan, Q., & Merrett, M. J. (1994). Extra- and intra-cellular carbonic anhydrase in relation to culture age in a high-calcifying strain of *Emiliania huxleyi* Lohmann. *New Phytologist*, *126*(4), 601–607. https://doi.org/10.1111/j.1469-8137.1994.tb02954.x

Nimer, N. A., Iglesias-Rodriguez, M. D., & Merrett, M. J. (1997). Bicarbonate utilization by marine phytoplankton species. *Journal of Phycology*, *33*(4), 625–631. https://doi.org/10.1111/j.0022-3646.1997.00625.x

Nimer, N. A., Ling, M. X., Brownlee, C., & Merrett, M. J. (1999). Inorganic carbon limitation, exofacial carbonic anhydrase activity, and plasma membrane redox activity in marine phytoplankton species. *Journal of Phycology*, *35*(6), 1200–1205. https://doi.org/10.1046/j.1529-8817.1999.3561200.x

Nimer, N. A., Warren, M., & Merrett, M. J. (1998). The regulation of photosynthetic rate and activation of extracellular carbonic anhydrase under CO_2-limiting conditions in the marine diatom *Skeletonema costatum*. *Plant, Cell and Environment*, *21*(8), 805–812. https://doi.org/10.1046/j.1365-3040.1998.00321.x

Pasciak, W. J., & Gavis, J. (1975). Transport limited nutrient uptake rates in *Ditylum brightwellii*. *Limnology and Oceanography*, *20*(4), 604–617. https://doi.org/10.4319/lo.1975.20.4.0604

Raven, J. A., & Falkowski, P. G. (1999). Oceanic sinks for atmospheric CO_2. *Plant, Cell and Environment*, *22*(6), 741–755. https://doi.org/10.1046/j.1365-3040.1999.00419.x

Raven, J. A., Walker, D. I., Johnston, A. M., Handley, L. L., & Kubler, J. E. (1995). Implications of C-13 natural abundance measurements for photosynthetic performance by marine macrophytes in their natural environment. *Marine Ecology Progress Series*, *123*(1–3), 193–206. https://doi.org/10.3354/meps123193

Reinfelder, J. R. (2011). Carbon concentrating mechanisms in eukaryotic marine phytoplankton. *Annual Review of Marine Science*, *3*(1), 291–315. https://doi.org/10.1146/annurev-marine-120709-142720

Revsbech, N. P., Jbrgensen, B. B., & Brix, O. (1981). Primary production oxygen microprofile. *Science*, *26*(4), 717–730.

Riebesell, U., Wolf-Gladrow, D. A., & Smetacek, V. (1993). Carbon dioxide limitation of marine phytoplankton growth rates. *Nature*, *361*(6409), 249–251.

Roberts, C. D., Palmer, M. D., Allan, R. P., Desbruyeres, D. G., Hyder, P., Liu, C., & Smith, D. (2016). Surface flux and ocean heat transport convergence contributions to seasonal and interannual variations of ocean heat content. *Journal of Geophysical Research: Oceans*, *121*(5), 3010–3028. https://doi.org/10.1002/2016JC012278.Received

Rost, B., Richter, K. U., Riebesell, U., & Hansen, P. J. (2006). Inorganic carbon acquisition in red tide dinoflagellates. *Plant, Cell and Environment*, *29*(5), 810–822. https://doi.org/10.1111/j.1365-3040.2005.01450.x

Rost, B., Riebesell, U., Burkhardt, S., & Sültemeyer, D. (2003). Carbon acquisition of bloom-forming marine phytoplankton. *Limnology and Oceanography*, *48*(1), 55–67. https://doi.org/10.4319/lo.2003.48.1.0055

Ryther, J. H. (1956). Photosynthesis in the ocean as a function of light intensity. *Limnology and Oceanography*, *1*(1), 61–70. https://doi.org/10.4319/lo.1956.1.1.0061

Samukawa, M., Shen, C., Hopkinson, B. M., & Matsuda, Y. (2014). Localization of putative carbonic anhydrases in the marine diatom, *Thalassiosira pseudonana*. *Photosynthesis Research*, *121*(2–3), 235–249. https://doi.org/10.1007/s11120-014-9967-x

Schubert, H., & Forster, R. M. (1997). Sources of variability in the factors used for modelling primary productivity in eutrophic waters. *Hydrobiologia*, *349*(1–3), 75–85. https://doi.org/10.1023/a:1003097512651

Shen, C., & Hopkinson, B. M. (2015). Size scaling of extracellular carbonic anhydrase activity in centric marine diatoms. *Journal of Phycology*, *51*(2), 255–263. https://doi.org/10.1111/jpy.12269

Smith-Harding, T. J., Beardall, J., & Mitchell, J. G. (2017). The role of external carbonic anhydrase in photosynthesis during growth of the marine diatom *Chaetoceros muelleri*. *Journal of Phycology*, *53*(6), 1159–1170. https://doi.org/10.1111/jpy.12572

Sunda, W. G., & Huntaman, S. A. (1997). Interrelated influence of iron, light and cell size on marine phytoplankton growth. *Nature*, *390*(6658), 389–392. https://doi.org/10.1038/37093

Tortell, P. D. (2000). Evolutionary and ecological perspectives on carbon acquisition in phytoplankton. *Limnology and Oceanography*, *45*(3), 744–750. https://doi.org/10.4319/lo.2000.45.3.0744

Trimborn, S., Lundholm, N., Thoms, S., Richter, K. U., Krock, B., Hansen, P. J., & Rost, B. (2008). Inorganic carbon acquisition in potentially toxic and non-toxic diatoms: The effect of pH-induced changes in seawater carbonate chemistry. *Physiologia Plantarum*, *133*(1), 92–105. https://doi.org/10.1111/j.1399-3054.2007.01038.x

Trimborn, S., Wolf-Gladrow, D., Richter, K. U., & Rost, B. (2009). The effect of pCO_2 on carbon acquisition and intracellular assimilation in four marine diatoms. *Journal of Experimental Marine Biology and Ecology*, *376*(1), 26–36. https://doi.org/10.1016/j.jembe.2009.05.017

Tsuji, Y., Nakajima, K., & Matsuda, Y. (2017). Molecular aspects of the biophysical CO_2-concentrating mechanism and its regulation in marine diatoms. *Journal of Experimental Botany*, *68*(14), 3763–3772. https://doi.org/10.1093/jxb/erx173

Widdicombe, C. E., & Harbour, D. (2021). *Phytoplankton taxonomic abundance and biomass time-series at Plymouth Station L4 in the Western English Channel, 1992-2020*. NERC EDS British Oceanographic Data Centre NOC. https://doi.org/10.5285/c9386b5c-b459-782f-e053-6c86abc0d129

Wolf-Gladrow, D., & Riebesell, U. (1997). Diffusion and reactions in the vicinity of plankton: A refined model for inorganic carbon transport. *Marine Chemistry*, *59*(1–2), 17–34. https://doi.org/10.1016/S0304-4203(97)00069-8

Wu, Y., Campbell, D. A., Irwin, A. J., Suggett, D. J., & Finkel, Z. V. (2014). Ocean acidification enhances the growth rate of larger diatoms. *Limnology and Oceanography*, *59*(3), 1027–1034. https://doi.org/10.4319/lo.2014.59.3.1027

Wu, Y., Jeans, J., Suggett, D. J., Finkel, Z. V., & Campbell, D. A. (2014). Large centric diatoms allocate more cellular nitrogen

to photosynthesis to counter slower RUBISCO turnover rates. *Frontiers in Marine Science*, *1*(DEC), 1–11. https://doi.org/10.3389/fmars.2014.00068

Yan, D., Beardall, J., & Gao, K. (2018). Variation in cell size of the diatom *Coscinodiscus granii* influences photosynthetic performance and growth. *Photosynthesis Research*, *137*(1), 41–52. https://doi.org/10.1007/s11120-017-0476-6

Zeebe, R., & Wolf-Gladrow, D. (2001). *CO_2 in seawater: Equilibrium, kinetics, isotopes*. Elsevier.

Zhang, Q., & Luo, Y. W. (2022). A competitive advantage of middle-sized diatoms from increasing seawater CO_2. *Frontiers in Microbiology*, *13*(May), 1–13. https://doi.org/10.3389/fmicb.2022.838629

SUPPORTING INFORMATION

Additional supporting information can be found online in the Supporting Information section at the end of this article.

Appendix S1: Contains Tables S1 and S2, Figures S1–S7, and the method for enriching seawater with CO_2 and calculation of inorganic carbon system parameters.

How to cite this article: Keys, M., Hopkinson, B., Highfield, A., Chrachri, A., Brownlee, C., & Wheeler, G. L. (2023). The requirement for external carbonic anhydrase in diatoms is influenced by the supply and demand for dissolved inorganic carbon. *Journal of Phycology*, *00*, 1–17. https://doi.org/10.1111/jpy.13416